HHS Public Access

Author manuscript

Cancer Cell. Author manuscript; available in PMC 2017 September 12.

Published in final edited form as:

Cancer Cell. 2016 September 12; 30(3): 432–443. doi:10.1016/j.ccell.2016.08.002.

An Osteopontin/CD44 axis in RhoGDI2-mediated metastasis suppression

Mansoor Ahmed[1,8,*], **Joseph L. Sottnik**[2], **Garrett M. Dancik**[3], **Divya Sahu**[4], **Donna Hansel**[4], **Dan Theodorescu**[2,5,6,*], and **Martin A. Schwartz**[1,7,*]

[1]Department of Internal Medicine (Cardiology), Yale Cardiovascular Research Center, Yale University, New Haven, CT 06520

[2]Department of Surgery, University of Colorado, Aurora, CO, 80045

[3]Mathematics and Computer Science Department, Eastern Connecticut State University, Willimantic, CT, 06226

[4]Department of Pathology, University of California, San Diego, La Jolla, CA, 92093

[5]Department of Pharmacology, University of Colorado, Aurora, CO, 80045

[6]University of Colorado Comprehensive Cancer Center, Aurora, CO, 80045

[7]Departments of Cell Biology and Biomedical Engineering, Yale University, New Haven, CT 06520

Summary

RhoGDI2 specifically suppresses bladder cancer metastasis but not primary tumor growth, which involves tumor-associated macrophages. We report that macrophage-secreted osteopontin binds to CD44s on the tumor cells and promotes invasion and clonal growth. These effects are RhoGDI2-sensitive and require CD44s binding to the Rac GEF TIAM1. Osteopontin expression correlates with tumor aggressiveness and poor clinical outcome in patients. Inhibiting this pathway potently blocked lung and lymph node metastasis; however, primary tumors and established metastasis were less sensitive. Osteopontin-CD44s-TIAM1 promotes clonal growth in vitro but not at high cell density. These data identify osteopontin-CD44-TIAM1-Rac axis as a RhoGDI2-sensitive pathway and potential therapeutic target in bladder cancer metastasis. They also elucidate the mechanism behind RhoGDI2 specificity for metastasis over established tumors.

eTOC Blurb

[*]Correspondence: Mansoor Ahmed: mansoor.ahmed@yale.edu, mansoornccs@gmail.com; Martin A. Schwartz: martin.schwartz@yale.edu; Dan Theodorescu: dan.theodorescu@ucdenver.edu.
[8]Lead Contact

Author contributions: MA had the initial idea for the project and did all experimental work except for orthotopic, subcutaneous work (JS) and human pathology (DS and DH); GD carried out analysis of publically available clinical data; MAS provided guidance throughout the work; MAS and MA analyzed experimental data; MA drafted the manuscript; all authors contributed to editing of the manuscript; DT and MAS provided funding.

Ahmed et al. identify macrophage-secreted osteopontin as a critical mediator of bladder cancer cell invasion and clonal growth. The effect is mediated by RhoGDI2 and requires CD44s binding to Rac GEF TIAM1. Inhibiting this pathway specifically blocks the initial steps in bladder cancer metastasis.

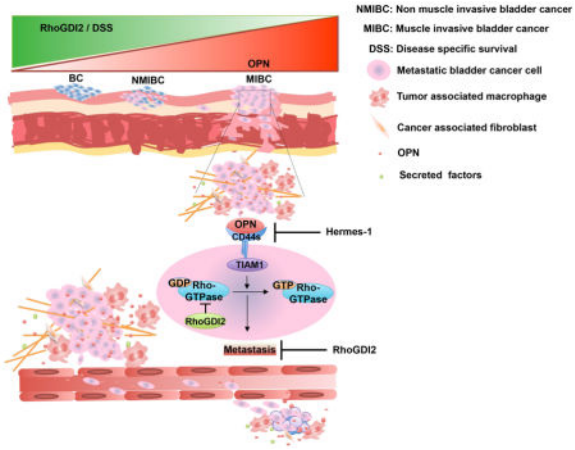

Introduction

Metastasis, the major cause of death in bladder cancer, is a multi-step process that involves cell invasion, migration and colonization of distant organs (Kaplan et al., 2014; Knowles and Hurst, 2014; Talmadge and Fidler, 2010). Rho GDP dissociation inhibitor 2 (RhoGDI2) has been identified as a specific bladder cancer metastasis suppressor (Gildea et al., 2002). Reduced expression of RhoGDI2 is associated with decreased survival of bladder cancer patients (Theodorescu et al., 2004) and studies in animal models showed that its re-expression specifically suppressed metastasis without affecting primary tumor growth or growth in culture (Gildea et al., 2002; Moissoglu et al., 2009). RhoGDI2 appears to suppress metastasis by modulating Rho GTPases signaling (Griner et al., 2014; Moissoglu et al., 2009).

The tumor microenvironment, consisting of extracellular matrix (ECM), fibroblasts, vasculature and tumor associated macrophages (TAMs), is critical for tumor growth and metastasis (Luga et al., 2012; Quail and Joyce, 2013). TAMs in particular are implicated in a RhoGDI2-sensitive pathway of bladder cancer metastasis (Said et al., 2012). Loss of RhoGDI2 in the tumor cells alters tumor cell-TAM crosstalk to enhance both local inflammation and tumor cell invasion and growth. This pathway involves secretion of versican by the tumor cells, which stimulates secretion of inflammatory cytokines by the macrophages, which act on the tumor cells to promote metastatic growth. However, major features of this cell-cell communication circuit are poorly understood. We therefore set out to understand more fully how RhoGDI2 controls tumor cell-macrophage crosstalk in bladder carcinoma metastasis.

Results

RhoGDI2 modulates invasion in response to macrophage-conditioned medium

These studies used the metastatic bladder cancer cell lines UMUC3 and T24T, and non-metastatic T24 and RT4. UMUC3 and T24T express negligible levels of RhoGDI2 compared to non-metastatic T24 and RT4 cells that express high levels of RhoGDI2 (Theodorescu et al., 2004; Titus et al., 2005). These cells represent the genomic fingerprint of human cancer and have been found to correlate well with clinical behavior (Dancik et al., 2011). Re-expression of RhoGDI2 strongly inhibited experimental metastasis while having little effect on the primary tumor growth (Moissoglu et al., 2009; Titus et al., 2005). In UMUC3 cells, RhoGDI2 expression had no effect on cell invasion through basement membrane protein (matrigel) under basal conditions (Figure 1A, B & C). However, cell invasion was stimulated by co-culture with Raw 264.7 macrophages, which was almost completely suppressed by RhoGDI2 (Figure 1B & C). Adding macrophage conditioned media (MCM) to untreated UMUC3 cells similarly induced invasion in a dose-dependent manner (Figure 1D), indicating that a secreted factor(s) mediated these effects. By contrast, macrophage-conditioned medium had no effect on transwell migration without the matrix coating (Figure S1A). Likewise, fibroblast (L cells) conditioned medium did not induce UMUC3 invasion (Figure S1B), suggesting cell type specificity.

To further investigate the RhoGDI2-dependence of these events, we prepared UMUC3 and T24T cells stably expressing RhoGDI2 or a defective GTPase-binding mutant, RhoGDI2D182R (Figure S6G) at the level of non-metastatic T24 cells (Figure S1C). Matrigel invasion assays showed that wild type (WT) RhoGDI2 suppressed macrophage-conditioned medium induced invasion while the D182R mutant was inactive (Figures 1E & S1D). However, RhoGDI2 did not affect serum-induced invasion (Figure 1F). To examine the generality of these findings and address whether loss of RhoGDI2 can be sufficient to induce invasion, RhoGDI2 was knocked down in non-metastatic RT4 cells. RhoGDI2 depletion conferred macrophage-conditioned medium induced invasion in these cells (Figure S1E, F). Together, these data show that RhoGDI2 specifically suppresses invasion stimulated by a macrophage-derived factor.

Osteopontin is the active factor in macrophage-conditioned medium

To identify the macrophage-derived tumor cell invasion-stimulating factor, we fractionated macrophage-conditioned medium. First, high-speed ultracentrifugation to distinguish soluble factor(s) from micro-vesicles showed that only the macrophage-conditioned medium supernatant induced invasion (Figure S2A). Macrophage-conditioned medium was then filtered using different molecular weight cut offs. These experiments showed no loss of activity after filtration through 3, 10, 30 and 50 kDa filters but a dramatic loss with a 100 kDa molecular weight cut off (Figure S2B). This result suggested a soluble factor in a range of 50–100 kDa. Osteopontin (OPN) is one of the macrophage-secreted molecules (Takahashi et al., 2000). Its' molecular weight is approximately 65 kDa, which falls within experimental range of 50–100 kDa for a potential active factor. It is also implicated in tumor growth and metastasis (Ahmed et al., 2011; Ahmed and Kundu, 2010). This prompted us to test its presence in macrophage-conditioned medium. Raw 264.7 macrophage conditioned medium

showed time dependent OPN protein secretion (Figure S2C), which quantitative ELISA showed reached ~3 μg/ml after 24 hr (Figure S2D).

To investigate whether OPN is the active component in macrophage-conditioned medium, we depleted OPN from macrophage-conditioned medium using control or anti-OPN IgG. This procedure removed 69% of the OPN (Figure 2A, B) and reduced macrophage-conditioned medium induced UMUC3 invasion by 68% (Figure 2C). Furthermore, transducing Raw 264.7 cells with OPN shRNA (Figure S2E), which decreased OPN secretion by approximately 70%, inhibited invasion to a similar extent compared to control shRNA cells (Figure 2D). To test whether OPN was sufficient to induce bladder cancer cell invasion, assays were carried out with recombinant OPN. Both mouse and human OPN stimulated invasion of UMUC3 cells in a dose-dependent manner (Figure S2F). Lastly, expression of WT but not mutant RhoGDI2 strongly suppressed OPN-induced invasion in UMUC3 and T24T cells, while knock down of RhoGDI2 in RT4 cells increased OPN induced invasion (Figures 2E, F & S2G). Together, these data show that OPN is the major factor in macrophage-conditioned medium that promotes RhoGDI2-sensitive bladder cancer cell invasion.

OPN expression and clinical outcomes in patients

In order to assess clinical relevance, we looked at five bladder cancer patient cohorts (total n = 633) where OPN was profiled in whole tissue from both tumors and normal bladder. In all cohorts, OPN expression was significantly up-regulated in muscle invasive tumor tissue compared to normal bladder tissue (Figure 3A–E, FC of 2.64 – 9.34, $p < 0.001$). In the two patient cohorts that included information about disease-specific survival, high expression correlated with poorer outcomes, which was statistically significant in the CNUH cohort (Figure 3F, HR = 2.31, $p = 0.028$). In the MSKCC cohort, a similar trend was observed but did not reach statistical significance (Figure 3G, HR = 1.91, $p = 0.062$), possibly due in part to lower n (165 vs. 87). We further investigated human specimens for correlations between metastasis and both OPN expression and macrophage infiltration. OPN staining in metastatic tumors (both the primary tumors and the corresponding lymph node metastases from the same patient) was significantly increased relative to non-metastatic primary tumors ($p<0.001$; Figures 3H,J & S3A). Macrophage infiltration (CD68 expression) followed a similar pattern (Figures 3I,J & S3B). The increase in macrophage content and OPN expression with tumor progression and poor prognosis are consistent with a role for OPN in bladder cancer metastasis.

CD44 mediates OPN-induced invasion

OPN signals through receptors that include CD44 and several integrins (Weber et al., 1997). To determine which receptor mediates UMUC3 invasion, cells were pre-treated with control IgG or function blocking IgG against CD44 (Siiskonen et al., 2014), integrins $\alpha_v\beta_3$ (Ahmed and Kundu, 2010), β1 or β4 (Oh et al., 2005). Anti-CD44 antibody potently inhibited macrophage-conditioned medium induced invasion whereas none of the integrin antibodies had any effect (Figure 4A). Western blot analysis, using Hela cells that express substantial levels of CD44 for comparison, showed that UMUC3 cells express high levels of CD44, which was unaffected by expression of WT or mutant RhoGDI2 (Figure 4B). The CD44

blocking antibody also blocked UMUC3 and T24T cells invasion in response to recombinant OPN (Figure 4C, D & E). Thus, CD44 appears to be the critical OPN receptor in this pathway.

The *CD44* gene contains 20 exons, with exons 1–5 found in all isoforms except the soluble isoform, CD44sol. The standard isoform (CD44s) consists of exons 1–5, 16–18 and 20 (Williams et al., 2013), with longer isoforms containing variable insertions of exons 6–15 (Figure S4A). To investigate the splice isoforms in UMUC3 cells, we carried out polymerase chain reactions (PCR) using primers that give products of different sizes for every transcript (Figure S4A). These primers gave a product of 669 bp, which represents transcript variants four or eight (Figure S4B). When cDNA isolated from UMUC3 cells was amplified using PCR primers specific for transcript variant four (CD44s), it gave the expected 714 bp product (Figure S4C). Thus, UMUC3 cells express CD44s.

To test its function, we constructed an shRNA-resistant CD44s-GFP rescue vector from the UMUC3 cDNA library. Its transduction into CD44 shRNA knock down cells and FACS sorting yielded cells where the transgene was expressed at high levels (Figure S5A). Re-expression of CD44s fully rescued macrophage-conditioned medium induced invasion in knockdown cells (Figure 4F). Together, these experiments identify CD44s as the critical OPN receptor that mediates bladder cancer cell invasion.

Interaction of TIAM1 with CD44s mediates OPN induced invasion

The cytoplasmic tail of CD44s interacts with the Rac guanine nucleotide exchange factor (GEF) T cell lymphoma antigen (TIAM1) (Bourguignon et al., 2000; Terawaki et al., 2010). TIAM1 activates the Rac subfamily of Rho GTPases and its expression is associated with lymph node metastasis in lung adenocarcinoma (Liu et al., 2014). The role of RhoGDI2 and involvement of Rho GTPases in invasion and metastasis (Magi et al., 2014) led us to test this pathway. Stable depletion of TIAM1 with shRNA in UMUC3 cells (Figure 5A) strongly inhibited invasion in response to both macrophage-conditioned medium and OPN (Figures 5B & C). To test more specifically whether the TIAM1 interaction with CD44 is necessary for invasion, we made point mutations in the CD44s rescue vector to reduce its affinity for TIAM1 (CD44s-E335K/E338K-GFP) (Terawaki et al., 2010) (Figure S5B). In stable CD44 knockdown cells reconstituted with WT or mutant CD44s-GFP at equivalent levels (Figure S5A), only WT CD44s rescued invasion (Figures 5D, E and S5C). These data show that the interaction of CD44s with TIAM1 is required for OPN-stimulated invasion. To ascertain the biochemical link between TIAM1 and RhoGDI2, we examined Rac1 activity. Both macrophage-conditioned medium and OPN activated Rac1 (Figure S6A, B), which was inhibited by CD44 knock down and rescued by WT but not with mutant CD44 (Figure S6C, D). Further, these effects were blocked with WT but not the Rac-binding defective RhoGDI2 mutant (Figure S6E, F & G). Together, these data establish a RhoGDI2-sensitive, OPN-CD44-TIAM1 pathway that activates Rac1 to promote bladder cancer invasion.

Effect on clonal cell growth

Clonal cell growth, the ability of a single cell to expand after colonizing a distant site, is a critical step in metastasis (Brady et al., 2016; Fidler, 1990; Fiebig et al., 2004; Malanchi et

al., 2012; Matano et al., 2015). We therefore examined whether the OPN-CD44-TIAM1 pathway governs this behavior. When UMUC3 cells were plated at single cell density, macrophage-conditioned medium showed potent, dose-dependent stimulation of colony formation (Figure 6A, B). Both OPN knockdown in the macrophages and antibody depletion of OPN inhibited this effect in UMUC3 (Figure 6C, D) and T24T cells (Figure 6E). Function blocking anti-CD44 antibody also blocked macrophage-conditioned medium induced clonal growth in both cell lines (Figures 7A, B, & S7A, B), as did knockdown of CD44, which was rescued by WT CD44s but not the TIAM1-binding mutant (Figures 7C & S7C). Knockdown of TIAM1 also inhibited macrophage-conditioned medium stimulated clonal growth (Figures 7D and S7D). Lastly, we tested the role of RhoGDI2. Expression of WT but not mutant RhoGDI2 suppressed macrophage-conditioned medium induced clonal growth in UMUC3 (Figures 7E and S7E) and T24T cells (Figure S7F, G).

To test whether loss of RhoGDI2 is sufficient to permit invasive but non-metastatic T24 cells to form colonies after stimulation with OPN, we stably depleted RhoGDI2 in these cells. Remarkably, RhoGDI2 knockdown conferred macrophage-conditioned medium and OPN-dependent clonal growth (Figures 7F and S7H, I). Together, these data provide strong evidence that the RhoGDI2-sensitive, OPN-CD44-TIAM1 pathway governs clonal growth in bladder cancer.

CD44 regulates metastasis

To determine whether CD44 governs metastasis in vivo, we assayed experimental lung metastasis after lateral tail vein injection of tumor cells. Stable knockdown of CD44 in UMUC3 cells strongly suppressed lung metastasis in this model. Over-expression of WT CD44s-GFP but not the TIAM1-binding mutant, not only rescued but also increased metastasis to levels well above the parent cell line, consistent with the higher CD44 expression in these cells (Figures 8A,D and S5A). We also tested the effect of the CD44 function-blocking antibody hermes-1 (Figure S8A). Co-injection of anti-CD44 IgG with the UMUC3 cells, with antibody injections continuing for the duration of the experiment, inhibited metastasis by 96.7% (Figure 8B). To confirm these results, we also examined an orthotopic model in which tumors in the bladder wall metastasize to draining lymph nodes (Muramaki et al., 2004). Expression of WT but not mutant CD44s potently controlled metastasis in this model (Figure 8C).

To determine whether the CD44 pathway was required only for the initial establishment of metastasis or their continued expansion, we also tested a protocol in which antibody injections were started 1 week after cell injection. Under this condition, metastasis was reduced by 63% (Figure 8B), much less than when co-injected. This result prompted us to re-examine cell growth, this time using cells plated at higher density where growth is no longer clonal. In these assays, macrophage-conditioned medium was only weakly stimulatory (Figure S8C). Growth at normal density is also independent of RhoGDI2 (Gildea et al., 2002). We then tested tumor growth in vivo. CD44 knock down or rescue with WT or mutant CD44 did not cause any significant changes in growth of the primary subcutaneous (Figure S8D) or orthotopic tumors (Figure S8B). We conclude that a

RhoGDI2-sensitive OPN-CD44-TIAM1-Rac1 pathway is critical for the initial steps in bladder cancer metastasis but less so for growth of established metastasis.

Discussion

In this study, we observed that RhoGDI2 specifically controls cell invasion stimulated by macrophage-conditioned medium. Interestingly, clonal cell growth was also stimulated by macrophage-conditioned medium and inhibited by RhoGDI2, thus, identifying a second step in metastasis that is governed by this pathway. OPN was identified as the critical mediator of cell invasion and colony formation based on shRNA-mediated knockdown of OPN in the macrophages, by antibody depletion of the macrophage-conditioned medium, and by direct stimulation with recombinant OPN. Although we cannot exclude other minor factors, the close correspondence between the reduction in OPN levels and cell invasion indicates that OPN is the major invasion/clonal growth stimulator produced by macrophages. Bioinformatic analysis and Immunohistochemistry of human patient samples also showed that OPN levels increase in muscle invasive/metastatic tumors compared to non-invasive/ non-metastatic tumors and normal tissue.

OPN is an ECM-associated, cytokine-like molecule that promotes tumor growth and metastasis in number of systems (Ahmed et al., 2011; Ahmed and Kundu, 2010; Chanmee et al., 2014; Joyce and Pollard, 2009; Rao et al., 2013; Rittling and Chambers, 2004; Wai and Kuo, 2004). OPN levels increase during cancer progression and high OPN is a marker of poor prognosis in bladder cancer (Ang et al., 2005; Zaravinos et al., 2011; Zaravinos et al., 2012). Thus, the identification of OPN as the key macrophage-derived factor that stimulates metastasis correlates well with its known properties.

Both shRNA-mediated knockdown and blocking antibody experiments identified CD44 as the OPN receptor that stimulates invasion and clonal growth. CD44s is the major isoform expressed in UMUC3 cells, and was able to fully rescue CD44 knockdown. Interestingly, transcriptome analysis of recurrent muscle invasive bladder cancer patients compared to newly diagnosed patients revealed increased CD44 expression (Choi et al., 2014; Zhang et al., 2014). Moreover, we found that TIAM1, which binds the CD44s cytoplasmic domain and functions as a GEF for Rac1 (Terawaki et al., 2010), is the critical intracellular effector required for stimulation of invasion. Indeed, OPN stimulation activated Rac1, which required TIAM1 and CD44, and was blocked by RhoGDI2. Thus, elucidation of the OPN-CD44-TIAM1-Rac1 axis provides a logical connection to the known function of RhoGDI2 as a regulator of Rho GTPases. In addition to UMUC3 and T24T cells, consistent effects were also observed in non-metastatic T24 and RT4 cells that express high levels of RhoGDI2. Together with the human gene expression data for OPN and CD44, these results provide strong evidence that the RhoGDI2-sensitive OPN-CD44-TIAM1-Rac1 pathway is generally relevant to human cancer (Figure 8E).

The stronger requirement for a RhoGDI2-sensitive OPN-CD44-TIAM1 pathway in the initial establishment of metastasis than for subsequent growth of established metastasis is very likely related to previous observations that RhoGDI2 expression does not affect primary tumors or growth in culture. These in vivo findings correlate well with in vitro

results that OPN-CD44-TIAM1 signaling promotes RhoGDI2-sensitive clonal cell growth but has only slight effects on growth in denser cultures. One possible explanation for these observations is that bladder cancer cells might secrete a paracrine factor or factors that promote their survival and growth, which would require a critical cell density to reach sufficient concentrations. Thus, only at clonal densities would tumor cell survival and growth depend on macrophage-derived OPN. Tumor invasion toward macrophages would therefore place cells in a local environment that supports their further expansion. Identification of tumor cell-derived paracrine factors that support their growth in denser conditions could provide a means to sensitize established tumors to inhibition of this pathway.

These results identify two major clinically relevant directions for future work. First, many patients are diagnosed with non-invasive bladder cancer and are treated with local chemotherapy, but tumors eventually progress to invasion and metastasis, which is incurable. The ~97% inhibition by anti-CD44 antibody in our experimental model suggests that blockade of the OPN-CD44-TIAM1-Rac1 pathway could be used to prevent metastasis in these patients. Second, identifying tumor cell-derived paracrine factors that support survival and growth under conditions of higher cell density may provide a path to combined therapy that would be effective in primary tumors or established metastasis.

Experimental procedures

Metastasis assays

For lung metastasis, stably transduced UMUC3 cell lines at 1×10^{6}/animal in 200 μl serum free medium were injected through the lateral tail veins into 6–8 week old athymic nude mice (nu/nu; Charles river). In some cases, UMUC3 cells were injected in medium containing with 50 μg hermes-1 antibody, with subsequent injections of 50 μg antibody twice/week. An additional group of mice received antibody injections starting 1 week after initial injections. In all cases, after a total of six weeks, mice were euthanized and lungs dissected. For lymph node metastasis, 6–8 weeks of age nude mice were challenged intravesically with 5×10^{5} luciferase labeled UMUC3 cells via direct injection into the bladder wall. Briefly, mice were anesthetized with isoflurane, the surgical site cleaned, and a small incision made to expose and express the bladder. Tumor cells were injected directly into the bladder wall. The peritoneum and cutaneous tissues were closed and mice treated with Buprenorphine SR (0.5 mg/kg) for pain management. Mice were recovered on room air. Luciferase signal was measured to determine tumor burden. Mice were euthanized 4 weeks after tumor challenge. Lumbo-sacral (retroperitoneal) and inguinal lymph nodes, which were in close vicinity and difficult to differentiate from orthotopic tumor luciferase signal, were harvested for all mice and pooled to investigate metastatic burden with qPCR (Cheng et al., 2013; Muramaki et al., 2004). Genomic DNA was isolated using a Qiagen kit (69504). To assess metastasis, nested qPCR for human chromosome 12p was performed (Nicholson et al., 2004; Nitz et al., 2008). 1 μg genomic DNA was amplified with 100 nM primer sets one; forward (5′ CTGACAGACAACCTTGCTCACTCAC 3′) and reverse (5′ AGGGAGTGCAGTGTGTCACTCTAGC 3′) for 8 cycles in 20 μl reaction. 1 μl from the first PCR reaction was used with 200 nM second set of primer; forward (5′

TGACCCTGATAAAGTTTCTTGGAA 3′) and reverse (5′ GGGACAGACACTGAGCCTTGAG 3′) to amplify the final product. Genomic DNA from without injected nude mice was used as negative control for qPCR. Human and mouse actin specific primers forward (5′ ATCATTGCTCCTCCTGAGCGC 3′) and reverse (5′ TACTCCTGCTTGCTGATCCA 3′) were used to amplify the actin as reference. Lung metastasis experiments were performed with the approval of IACUC at Yale University. Lymph node metastasis experiment was performed with the approval of IACUC at University of Colorado.

Subcutaneous tumor growth assay

6–8 weeks of age nude mice were used for the experiments. Mice were challenged subcutaneously with 5×10^5 UMUC3 cells per site, 4 sites per mouse. Tumors were measured twice weekly using calipers and volume determined using the formula: $V = (S^2 \times L)/2$ where V=volume, S=shortest diameter, and L=longest diameter. The volumes of 4 tumor sites were averaged across each mouse. Measurements were normalized per group to values 7 days after tumor challenge. This experiment was performed with the approval of IACUC at University of Colorado.

Gene expression datasets

We carried out a comprehensive search of the Gene Expression Omnibus (GEO) (Barrett et al., 2011), Array Express (Rustici et al., 2013), and the literature, and identified all bladder cancer patient cohorts that contained normal bladder tissue samples and clinical information about patient stage. Five cohorts (n= 633) were identified: 55 patients profiled at Aarhus University Hospital, Skejby (AUH cohort (Dyrskjot et al., 2004), downloaded from GEO, accession #GSE3167); 62 patients profiled by Stransky and colleagues (Stransky cohort (Stransky et al., 2006), downloaded from Array Express, accession #E-TABM-147), 154 patients profiled by Lindgren and colleagues (Lindgren cohort (Lindgren et al., 2010), downloaded from GEO, accession #GSE19915), 233 patients profiled at Chungbuk National University Hospital (CNUH cohort (Kim et al., 2010) downloaded from GEO, accession #GSE13507), and 129 patients profiled at Memorial Sloan Kettering Cancer Center (MSKCC cohort (Sanchez-Carbayo et al., 2006) downloaded from supplemental material to publication). The processed data was downloaded and analyzed in all cases.

Patient specimens and TMA construction

Specimens included archived paraffin blocks from patients who underwent radical cystectomy or cystoprostatectomy for muscle-invasive UCC (pathological stage pT2 or greater). Primary bladder tumors that were used for analysis were either non-metastatic (n=60) or metastatic to regional lymph nodes (n=86). Paired lymph node metastases from the latter group were available in 73 cases for analysis. All specimens were re-reviewed by one of the authors (DH) for diagnostic accuracy, and three tumor regions per specimen were used for tissue microarray generation. This is study was approved by the UCSD Institutional Review Board with a waiver of consent granted.

Immunohistochemistry and Scoring

Slides were deparaffinized and rehydrated according to standard serial histo-clear and ethanol wash steps. For CD68, antigen retrieval was performed by Tris-EDTA buffer incubation [10 mM Tris base, 1 mM EDTA (pH 9.0)] using a household vegetable steamer for 20 min followed by cool down to room temperature for 10 min. No antigen retrieval was required for OPN. Slides were incubated either with CD68 antibody (1:50, clone PG-M1, Dako, Glostrup, Denmark) or OPN antibody (1:500, ab8848, Abcam, Cambridge, United Kingdom) overnight at 4°C. For immunohistochemical detection HRP-Polymer followed by DAB (Abcam) were used, and slides were subsequently counterstained with hematoxylin. Osteopontin immunostaining was scored semi-quantitatively using a range of 0 (no staining), 1 (weak staining), 2 (moderate staining) and 3 (intense staining). CD68 positive cells were scored semi-quantitatively as a percentage, in steps of 10%.

Statistical analyses

For gene expression analysis, probes were identified that corresponded to OPN (CNUH cohort) or its alternative name SPP1 (remaining cohorts). If multiple probes corresponded to the gene, then the probe with the highest mean expression was used. Fold-change (FC) was used to characterize the difference in expression between muscle invasive tumors and normal tumors. p-values were calculated using the non-parametric Wilcoxon Rank Sum test. We generated Kaplan-Meier curves for patients with low and high expression of OPN, using the median as the cut-point. Disease-specific survival was used as the endpoint. Hazard ratios and log-rank p-values were obtained using the coxph function in R. For human sample IHC analysis; p-values evaluating change in expression scores between matched samples (Met primary vs Mets) and independent samples (Non-met Primary vs. Met Primary and Non-met Primary vs. Mets) were calculated using the non-parametric Wilcoxon signed-rank test and the Wilcoxon rank-sum test, respectively. Other experiments were analyzed with one-way or two-way ANOVA and two-tailed unpaired t test.

Supplementary Material

Refer to Web version on PubMed Central for supplementary material.

Acknowledgments

This work was supported by USPHS grant RO1 CA143971 to MAS and DT, and RO1 47214 to MAS. All experiments presented involving the use of animals have been approved by Institutional Animal Care and Use Committee at Yale University and University of Colorado-Denver.

References

Ahmed M, Behera R, Chakraborty G, Jain S, Kumar V, Sharma P, Bulbule A, Kale S, Kumar S, Mishra R, et al. Osteopontin: a potentially important therapeutic target in cancer. Expert Opin Ther Targets. 2011; 15:1113–1126. [PubMed: 21718227]

Ahmed M, Kundu GC. Osteopontin selectively regulates p70S6K/mTOR phosphorylation leading to NF-kappaB dependent AP-1-mediated ICAM-1 expression in breast cancer cells. Molecular cancer. 2010; 9:101. [PubMed: 20459645]

Ang C, Chambers AF, Tuck AB, Winquist E, Izawa JI. Plasma osteopontin levels are predictive of disease stage in patients with transitional cell carcinoma of the bladder. BJU Int. 2005; 96:803–805. [PubMed: 16153205]

Barrett T, Troup DB, Wilhite SE, Ledoux P, Evangelista C, Kim IF, Tomashevsky M, Marshall KA, Phillippy KH, Sherman PM, et al. NCBI GEO: archive for functional genomics data sets--10 years on. Nucleic acids research. 2011; 39:D1005–1010. [PubMed: 21097893]

Bourguignon LY, Zhu H, Shao L, Chen YW. CD44 interaction with tiam1 promotes Rac1 signaling and hyaluronic acid-mediated breast tumor cell migration. J Biol Chem. 2000; 275:1829–1838. [PubMed: 10636882]

Brady JJ, Chuang CH, Greenside PG, Rogers ZN, Murray CW, Caswell DR, Hartmann U, Connolly AJ, Sweet-Cordero EA, Kundaje A, Winslow MM. An Arntl2-Driven Secretome Enables Lung Adenocarcinoma Metastatic Self-Sufficiency. Cancer Cell. 2016; 29:697–710. [PubMed: 27150038]

Chanmee T, Ontong P, Konno K, Itano N. Tumor-associated macrophages as major players in the tumor microenvironment. Cancers (Basel). 2014; 6:1670–1690. [PubMed: 25125485]

Cheng T, Roth B, Choi W, Black PC, Dinney C, McConkey DJ. Fibroblast growth factor receptors-1 and -3 play distinct roles in the regulation of bladder cancer growth and metastasis: implications for therapeutic targeting. PLoS One. 2013; 8:e57284. [PubMed: 23468956]

Choi W, Porten S, Kim S, Willis D, Plimack ER, Hoffman-Censits J, Roth B, Cheng T, Tran M, Lee IL, et al. Identification of distinct basal and luminal subtypes of muscle-invasive bladder cancer with different sensitivities to frontline chemotherapy. Cancer Cell. 2014; 25:152–165. [PubMed: 24525232]

Dancik GM, Ru Y, Owens CR, Theodorescu D. A framework to select clinically relevant cancer cell lines for investigation by establishing their molecular similarity with primary human cancers. Cancer research. 2011; 71:7398–7409. [PubMed: 22012889]

Dyrskjot L, Kruhoffer M, Thykjaer T, Marcussen N, Jensen JL, Moller K, Orntoft TF. Gene expression in the urinary bladder: a common carcinoma in situ gene expression signature exists disregarding histopathological classification. Cancer research. 2004; 64:4040–4048. [PubMed: 15173019]

Fidler IJ. Critical factors in the biology of human cancer metastasis: twenty-eighth G.H.A. Clowes memorial award lecture. Cancer research. 1990; 50:6130–6138. [PubMed: 1698118]

Fiebig HH, Maier A, Burger AM. Clonogenic assay with established human tumour xenografts: correlation of in vitro to in vivo activity as a basis for anticancer drug discovery. Eur J Cancer. 2004; 40:802–820. [PubMed: 15120036]

Gildea JJ, Seraj MJ, Oxford G, Harding MA, Hampton GM, Moskaluk CA, Frierson HF, Conaway MR, Theodorescu D. RhoGDI2 is an invasion and metastasis suppressor gene in human cancer. Cancer research. 2002; 62:6418–6423. [PubMed: 12438227]

Griner EM, Dancik GM, Costello JC, Owens C, Guin S, Edwards MG, Brautigan DL, Theodorescu D. RhoC is an Unexpected Target of RhoGDI2 in Prevention of Lung Colonization of Bladder Cancer. Mol Cancer Res. 2014

Joyce JA, Pollard JW. Microenvironmental regulation of metastasis. Nat Rev Cancer. 2009; 9:239–252. [PubMed: 19279573]

Kaplan AL, Litwin MS, Chamie K. The future of bladder cancer care in the USA. Nat Rev Urol. 2014; 11:59–62. [PubMed: 23979659]

Kim WJ, Kim EJ, Kim SK, Kim YJ, Ha YS, Jeong P, Kim MJ, Yun SJ, Lee KM, Moon SK, et al. Predictive value of progression-related gene classifier in primary non-muscle invasive bladder cancer. Molecular cancer. 2010; 9:3. [PubMed: 20059769]

Knowles MA, Hurst CD. Molecular biology of bladder cancer: new insights into pathogenesis and clinical diversity. Nat Rev Cancer. 2014; 15:25–41.

Lindgren D, Frigyesi A, Gudjonsson S, Sjodahl G, Hallden C, Chebil G, Veerla S, Ryden T, Mansson W, Liedberg F, Hoglund M. Combined gene expression and genomic profiling define two intrinsic molecular subtypes of urothelial carcinoma and gene signatures for molecular grading and outcome. Cancer research. 2010; 70:3463–3472. [PubMed: 20406976]

Liu S, Li Y, Qi W, Zhao Y, Huang A, Sheng W, Lei B, Lin P, Zhu H, Li W, Shen H. Expression of Tiam1 predicts lymph node metastasis and poor survival of lung adenocarcinoma patients. Diagn Pathol. 2014; 9:69. [PubMed: 24661909]

Luga V, Zhang L, Viloria-Petit AM, Ogunjimi AA, Inanlou MR, Chiu E, Buchanan M, Hosein AN, Basik M, Wrana JL. Exosomes mediate stromal mobilization of autocrine Wnt-PCP signaling in breast cancer cell migration. Cell. 2012; 151:1542–1556. [PubMed: 23260141]

Magi S, Takemoto Y, Kobayashi H, Kasamatsu M, Akita T, Tanaka A, Takano K, Tashiro E, Igarashi Y, Imoto M. 5-Lipoxygenase and cysteinyl leukotriene receptor 1 regulate epidermal growth factor-induced cell migration through Tiam1 upregulation and Rac1 activation. Cancer Sci. 2014; 105:290–296. [PubMed: 24350867]

Malanchi I, Santamaria-Martinez A, Susanto E, Peng H, Lehr HA, Delaloye JF, Huelsken J. Interactions between cancer stem cells and their niche govern metastatic colonization. Nature. 2012; 481:85–89.

Matano M, Date S, Shimokawa M, Takano A, Fujii M, Ohta Y, Watanabe T, Kanai T, Sato T. Modeling colorectal cancer using CRISPR-Cas9-mediated engineering of human intestinal organoids. Nat Med. 2015; 21:256–262. [PubMed: 25706875]

Moissoglu K, McRoberts KS, Meier JA, Theodorescu D, Schwartz MA. Rho GDP dissociation inhibitor 2 suppresses metastasis via unconventional regulation of RhoGTPases. Cancer research. 2009; 69:2838–2844. [PubMed: 19276387]

Muramaki M, Miyake H, Kamidono S, Hara I. Over expression of CD44V8–10 in human bladder cancer cells decreases their interaction with hyaluronic acid and potentiates their malignant progression. J Urol. 2004; 171:426–430. [PubMed: 14665947]

Nicholson BE, Frierson HF, Conaway MR, Seraj JM, Harding MA, Hampton GM, Theodorescu D. Profiling the evolution of human metastatic bladder cancer. Cancer research. 2004; 64:7813–7821. [PubMed: 15520187]

Nitz MD, Harding MA, Theodorescu D. Invasion and metastasis models for studying RhoGDI2 in bladder cancer. Methods Enzymol. 2008; 439:219–233. [PubMed: 18374168]

Oh JE, Kook JK, Min BM. Beta ig-h3 induces keratinocyte differentiation via modulation of involucrin and transglutaminase expression through the integrin alpha3beta1 and the phosphatidylinositol 3-kinase/Akt signaling pathway. J Biol Chem. 2005; 280:21629–21637. [PubMed: 15805105]

Quail DF, Joyce JA. Microenvironmental regulation of tumor progression and metastasis. Nat Med. 2013; 19:1423–1437. [PubMed: 24202395]

Rao G, Wang H, Li B, Huang L, Xue D, Wang X, Jin H, Wang J, Zhu Y, Lu Y, et al. Reciprocal interactions between tumor-associated macrophages and CD44-positive cancer cells via osteopontin/CD44 promote tumorigenicity in colorectal cancer. Clin Cancer Res. 2013; 19:785–797. [PubMed: 23251004]

Rittling SR, Chambers AF. Role of osteopontin in tumour progression. Br J Cancer. 2004; 90:1877–1881. [PubMed: 15138464]

Rustici G, Kolesnikov N, Brandizi M, Burdett T, Dylag M, Emam I, Farne A, Hastings E, Ison J, Keays M, et al. ArrayExpress update--trends in database growth and links to data analysis tools. Nucleic acids research. 2013; 41:D987–990. [PubMed: 23193272]

Said N, Sanchez-Carbayo M, Smith SC, Theodorescu D. RhoGDI2 suppresses lung metastasis in mice by reducing tumor versican expression and macrophage infiltration. J Clin Invest. 2012; 122:1503–1518. [PubMed: 22406535]

Sanchez-Carbayo M, Socci ND, Lozano J, Saint F, Cordon-Cardo C. Defining molecular profiles of poor outcome in patients with invasive bladder cancer using oligonucleotide microarrays. Journal of clinical oncology : official journal of the American Society of Clinical Oncology. 2006; 24:778–789. [PubMed: 16432078]

Siiskonen H, Karna R, Hyttinen JM, Tammi RH, Tammi MI, Rilla K. Hyaluronan synthase 1 (HAS1) produces a cytokine-and glucose-inducible, CD44-dependent cell surface coat. Exp Cell Res. 2014; 320:153–163. [PubMed: 24099991]

Stransky N, Vallot C, Reyal F, Bernard-Pierrot I, de Medina SG, Segraves R, de Rycke Y, Elvin P, Cassidy A, Spraggon C, et al. Regional copy numberindependent deregulation of transcription in cancer. Nature genetics. 2006; 38:1386–1396. [PubMed: 17099711]

Takahashi F, Takahashi K, Maeda K, Tominaga S, Fukuchi Y. Osteopontin is induced by nitric oxide in RAW 264.7 cells. IUBMB Life. 2000; 49:217–221. [PubMed: 10868913]

Talmadge JE, Fidler IJ. AACR centennial series: the biology of cancer metastasis: historical perspective. Cancer research. 2010; 70:5649–5669. [PubMed: 20610625]

Terawaki S, Kitano K, Mori T, Zhai Y, Higuchi Y, Itoh N, Watanabe T, Kaibuchi K, Hakoshima T. The PHCCEx domain of Tiam1/2 is a novel proteinand membrane-binding module. EMBO J. 2010; 29:236–250. [PubMed: 19893486]

Theodorescu D, Sapinoso LM, Conaway MR, Oxford G, Hampton GM, Frierson HF Jr. Reduced expression of metastasis suppressor RhoGDI2 is associated with decreased survival for patients with bladder cancer. Clin Cancer Res. 2004; 10:3800–3806. [PubMed: 15173088]

Titus B, Frierson HF Jr, Conaway M, Ching K, Guise T, Chirgwin J, Hampton G, Theodorescu D. Endothelin axis is a target of the lung metastasis suppressor gene RhoGDI2. Cancer research. 2005; 65:7320–7327. [PubMed: 16103083]

Wai PY, Kuo PC. The role of Osteopontin in tumor metastasis. J Surg Res. 2004; 121:228–241. [PubMed: 15501463]

Weber GF, Ashkar S, Cantor H. Interaction between CD44 and osteopontin as a potential basis for metastasis formation. Proc Assoc Am Physicians. 1997; 109:1–9. [PubMed: 9010911]

Williams K, Motiani K, Giridhar PV, Kasper S. CD44 integrates signaling in normal stem cell, cancer stem cell and (pre)metastatic niches. Exp Biol Med (Maywood). 2013; 238:324–338. [PubMed: 23598979]

Zaravinos A, Lambrou GI, Volanis D, Delakas D, Spandidos DA. Spotlight on differentially expressed genes in urinary bladder cancer. PLoS One. 2011; 6:e18255. [PubMed: 21483670]

Zaravinos A, Volanis D, Lambrou GI, Delakas D, Spandidos DA. Role of the angiogenic components, VEGFA, FGF2, OPN and RHOC, in urothelial cell carcinoma of the urinary bladder. Oncol Rep. 2012; 28:1159–1166. [PubMed: 22895562]

Zhang S, Liu Y, Liu Z, Zhang C, Cao H, Ye Y, Wang S, Zhang Y, Xiao S, Yang P, et al. Transcriptome profiling of a multiple recurrent muscle-invasive urothelial carcinoma of the bladder by deep sequencing. PLoS One. 2014; 9:e91466. [PubMed: 24622401]

Significance

Metastasis is the major cause of death from bladder cancer. RhoGDI2 has been identified as a critical inhibitor of metastasis in bladder cancer but has little effect on growth of the primary tumor. We now report that RhoGDI2 inhibits responses of bladder cancer cells to osteopontin secreted by macrophages in the tumor microenvironment, which promotes bladder cancer invasion and clonal growth through CD44 and TIAM1. These events, however, are less important for growth of established tumors or higher density cultures. Elucidating this pathway identifies therapeutic targets for initial steps in metastasis and suggests a strategy for developing effective treatments for established metastasis.

Highlights

- RhoGDI2 inhibits macrophage stimulated bladder cancer invasion and clonal growth.
- Macrophage-secreted Osteopontin induces these effects via CD44 and Rac GEF TIAM1.
- This pathway is vital for initiation of metastasis but not for established tumors.

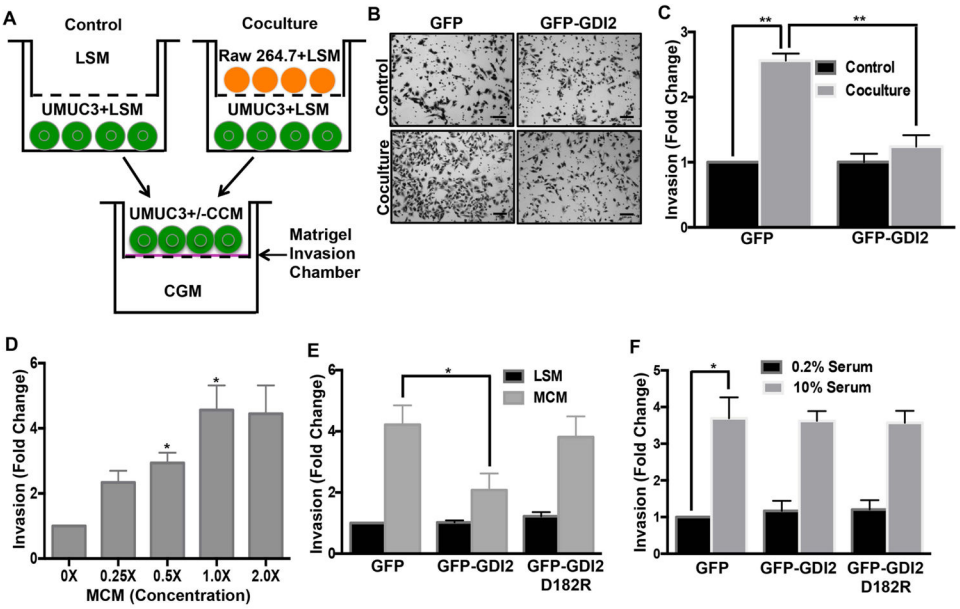

Figure 1. RhoGDI2 regulates macrophage-conditioned medium induced invasion of bladder cancer cells

(**A**) 1×10^5 UMUC3 cells were co-cultured with 3×10^5 Raw 264.7 cells for 18 hr; these "conditioned" UMUC3 cells were then seeded in matrigel invasion chambers in co-culture conditioned medium (CCM) and invasion analyzed after 7 hr. **(B)** Representative images of cells on the underside of the filter (scale bar, 100 μm) (**C**) Quantification of matrigel invasion. Values are mean ± SEM, fold change relative to control, n=3, **p < 0.01. (**D**) 4×10^4 UMUC3 were analyzed for invasion through matrigel for 18 hr with the indicated final concentration of macrophage-conditioned medium (MCM). Quantification of invasion from 5 different fields as in (C); n=3, *p < 0.05. (**E**) UMUC3 cells stably expressing GFP, WT GFP-RhoGDI2 or the D182R mutant were assayed for matrigel invasion in low serum medium (LSM: 0.2% FBS) or macrophage-conditioned medium and quantified as in (C). n=4; *p < 0.05. (**F**) UMUC3 cell stably expressing GFP, WT GFP-RhoGDI2 or the D182R mutant were assayed for matrigel invasion either in low (0.2% FBS) or high serum medium (10.0% FBS) for 22h. Quantified as in (C). n=3; *p < 0.05. See also Figure S1.

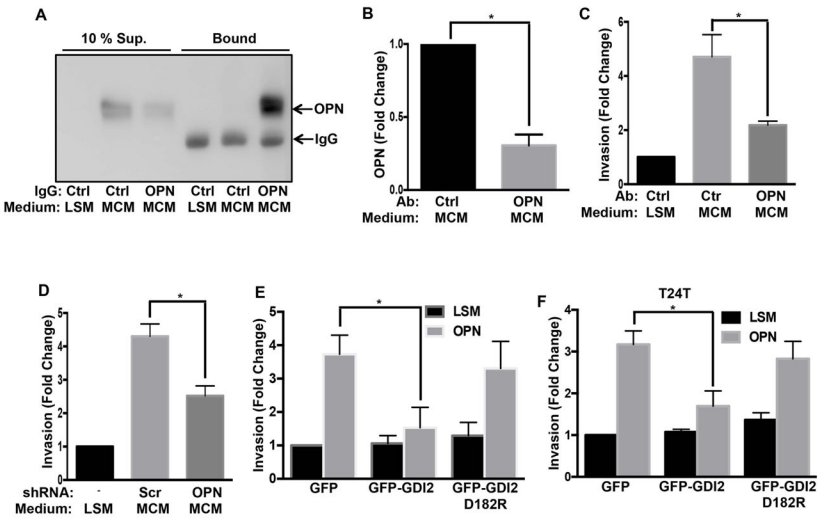

Figure 2. Osteopontin mediates macrophage-conditioned medium induced invasion

(**A**) Conditioned or unconditioned low serum medium was incubated with control or anti-OPN IgG on beads. Both supernatants and bound material were analyzed for OPN by western blotting. (**B**) Quantification of OPN depletion from (A), n=3. (**C**) Quantification of invaded UMUC3 cells with or without OPN depletion as in (A). Values are mean ± SEM, n=3, fold change relative to control, *p < 0.05. (**D**) Effect of OPN knockdown (Figure S2E) on UMUC3 invasion, quantified as in (C). n=3; *p < 0.05. (**E**) UMUC3 (**F**) T24T cells stably expressing GFP, GFP-WT RhoGDI2 or D182R mutant RhoGDI2 were analyzed for matrigel invasion in low serum medium (0.2% FBS) with or without 5 μg/ml recombinant mouse OPN for 18 hr, quantified as in (C), *p < 0.05. See also Figure S2.

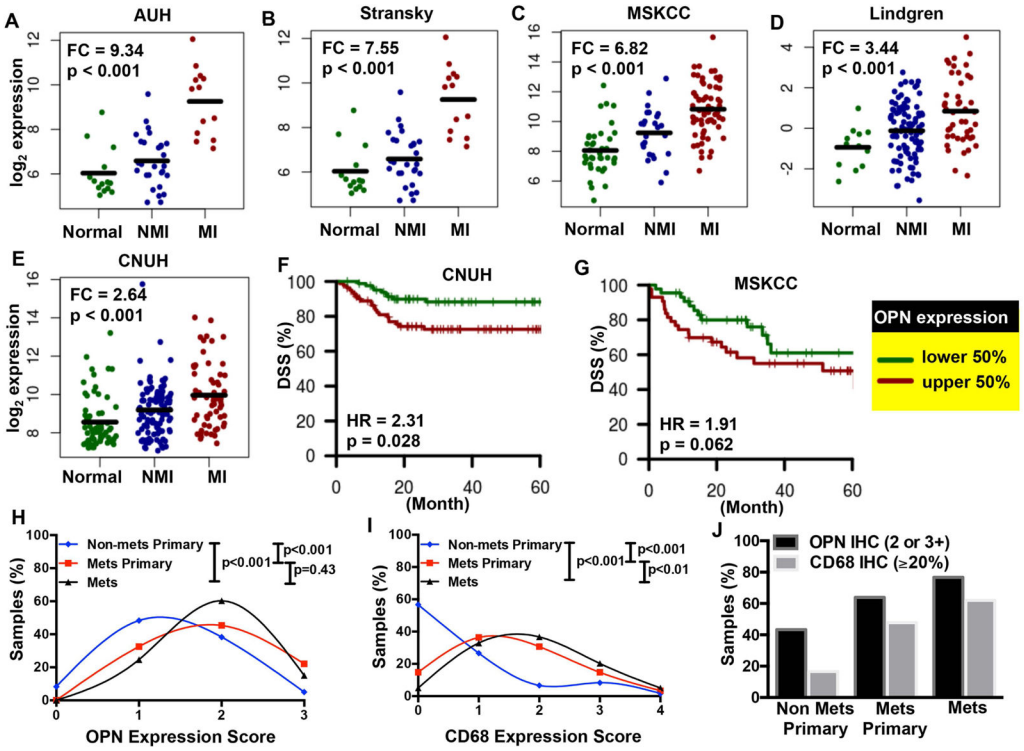

Figure 3. Osteopontin expression and clinical outcomes

Gene expression in normal bladder, non-muscle invasive (NMI) and muscle invasive (MI) bladder tumor tissue in the (**A**) AUH (n=55), (**B**) Stransky (n=62), (**C**) MSKCC (n=129), (**D**) Lindgren (n=154), and (**E**) CNUH (n=233) cohorts. Fold-change (FC) indicates expression in MI tumors relative to normal samples, with p-values calculated using the non-parametric Wilcoxon Rank-Sum test. Kaplan Meier curves were generated for patients with low and high levels of OPN expression, relative to the median, in (**F**) CNUH (n=165) and (**G**) MSKCC (n= 87) cohorts, with disease-specific survival (DSS) as the endpoint. The log-rank p-value is reported. Abbreviations: HR, hazard ratio. (**H & I**) OPN and CD68 staining in primary bladder tumors that were either non-metastatic (n=60) or metastatic to regional lymph nodes (n=86) with the paired lymph node metastases (n=73). % Positive (CD68) was converted to an expression score to match that of the OPN expression. (**J**) The percent of samples with positive expression of OPN (2 or 3+) and CD68 (≥20%) are depicted for non-metastatic primary tumors (non-met primary), metastatic primary tumors (met primary), and distal metastatic tumors (mets). See also Figure S3.

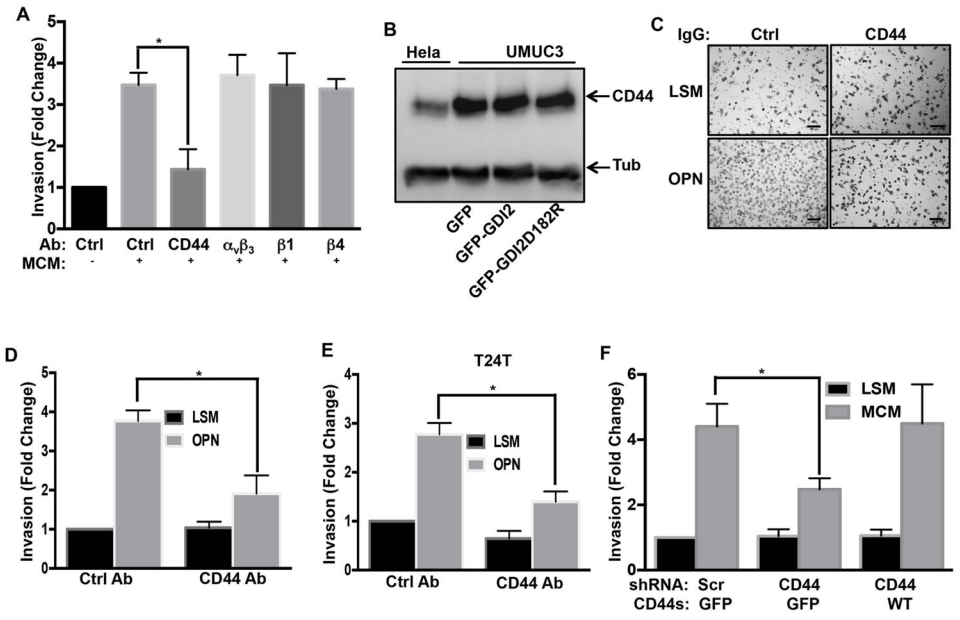

Figure 4. CD44 mediates OPN induced invasion

(**A**) Cells were pretreated with control antibody or function blocking antibodies to CD44 or integrins $\alpha_v\beta_3$, β1 or β4 antibody as described in experimental procedures. Matrigel invasion was assayed with or without macrophage-conditioned medium for 18 hr and analyzed as in Figure 1. Values represent fold change relative to control, n=3, *p < 0.05. (**B**) Lysates from Hela cells and the indicated stably transfected UMUC3 cells were analyzed by western blotting for CD44 or Tubulin (Tub) as a loading control. (**C**) Representative images from UMUC3 matrigel invasion assays with control or CD44 antibody, in low serum medium (LSM) with or without 5 μg/ml rmOPN (scale bar, 100 μm) (**D**) Quantification of (C), values are fold changes relative to control, n=3, *p < 0.05. (**E**) T24T cells with control or CD44 antibody were analyzed for invasion with or without 5 μg/ml rmOPN for 18 hr. Results quantified as in (D), n=3, *p < 0.05 (**F**) UMUC3 cells stably expressing scrambled or CD44 shRNA were reconstituted with GFP or CD44-GFP (expression in Figure S5A) as indicated. Invasion for 18 hr with or without macrophage-conditioned medium was assayed as in Figure 1, n=4, *p < 0.05. See also Figure S4 & S5.

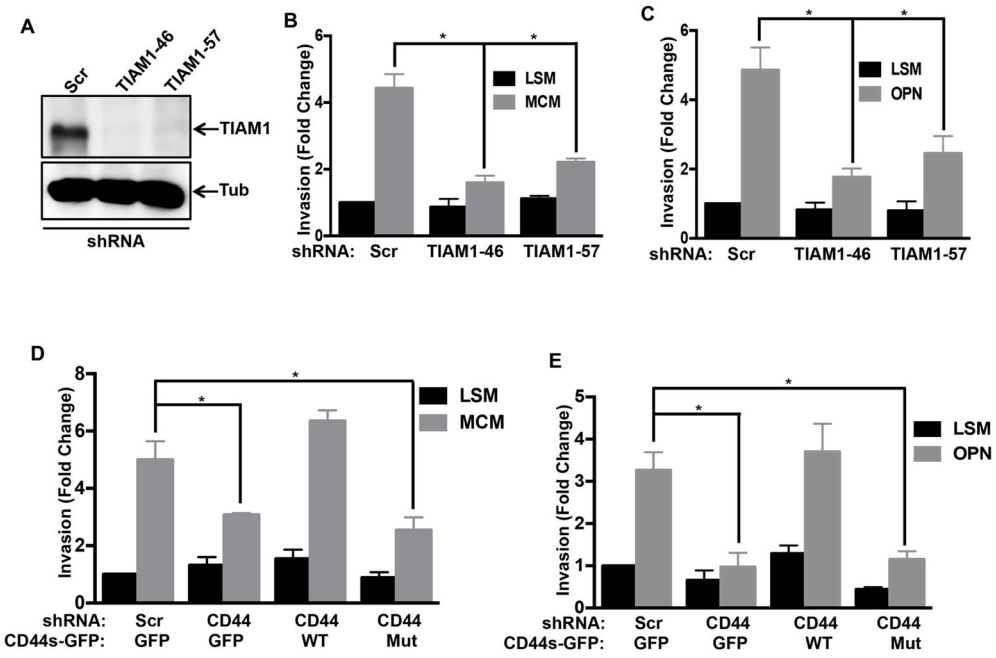

Figure 5. CD44s-TIAM1 interaction mediates OPN-Induced invasion

(**A)** Western blot for TIAM1 in scrambled and TIAM1 shRNA stable lines, with Tubulin (Tub) loading control. (**B&C**) UMUC3 cells stably expressing scrambled shRNA or two different TIAM1 shRNAs were analyzed for matrigel invasion either with macrophage-conditioned medium or 5 μg/ml recombinant mouse OPN. Values are mean ± SEM, fold change relative to control, n=3, *$p < 0.05$. (**D&E**) UMUC3 cells stably expressing the indicated constructs were analyzed for matrigel invasion either with macrophage-conditioned medium or OPN for 18 hr, n=3, *$p < 0.05$. See also Figure S5 and S6.

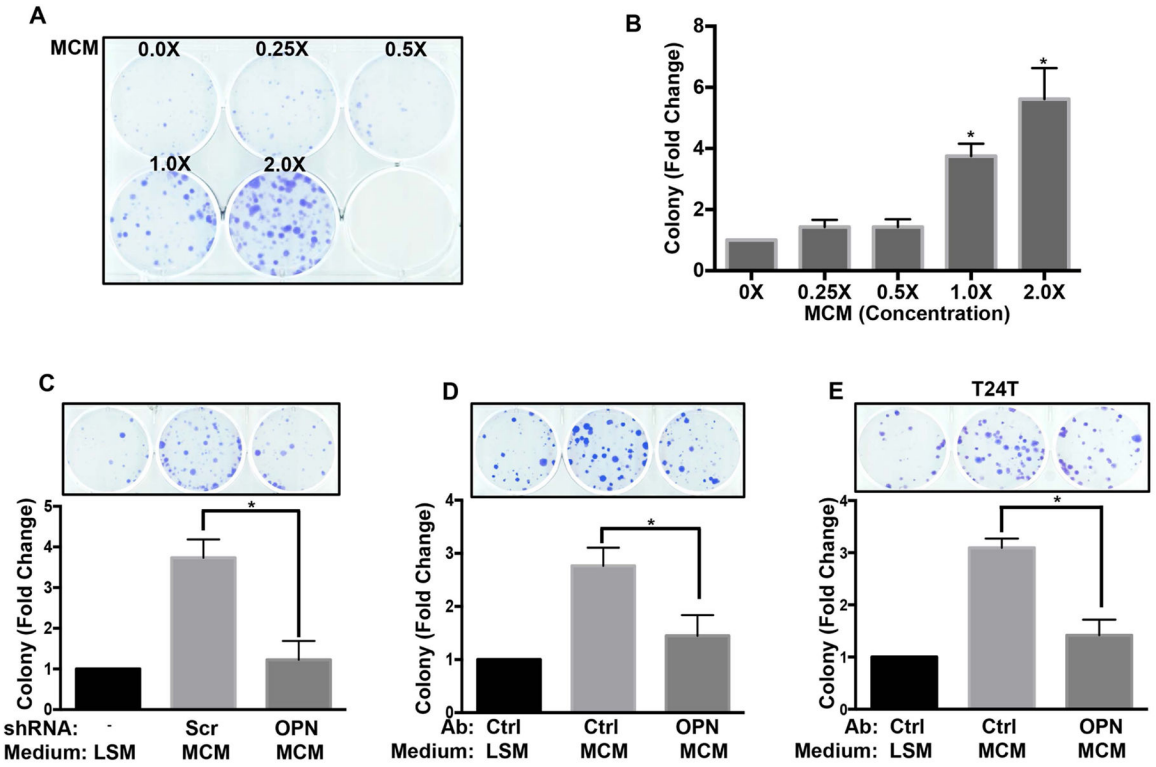

Figure 6. macrophage-conditioned medium potentiates clonal growth of bladder cancer cells

(**A**) 300 UMUC3 cells per well were seeded in 6-well plates with the indicated concentration of macrophage-conditioned medium in medium with 2% FBS. After 10 days, cells were fixed and stained. Shown is a representative image of the plates (**B**) Quantification of colony numbers from (A). Values are mean ± SEM, fold change relative to control, n=3, *p < 0.05. (**C**) UMUC3 colony assays as in (A) were done in macrophage-conditioned medium from stable scramble shRNA or OPN shRNA expressing Raw 264.7 cells. Quantification as in B, *p < 0.05. (**D**) UMUC3 (**E**) T24T colony assays were done as in (A) using control or OPN antibody depleted macrophage-conditioned medium. Quantification as in B, n=3, *p < 0.05.

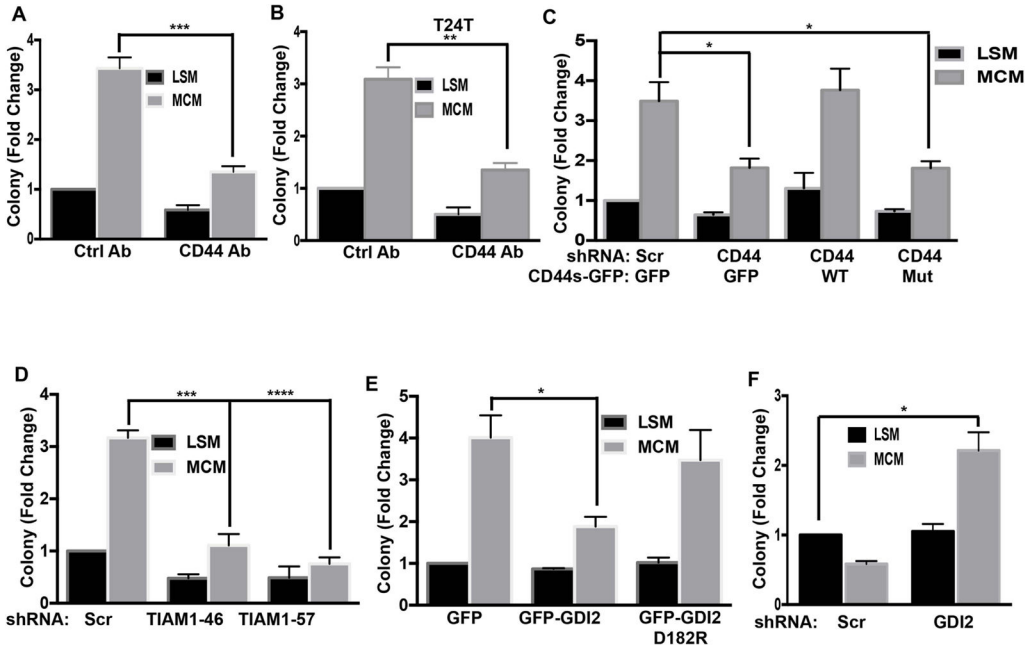

Figure 7. CD44/TIAM1/RhoGDI2 regulate macrophage-conditioned medium induce clonal growth

(**A**) UMUC3 cells pretreated with CD44 antibody were analyzed for clonal growth for 10 days as in Figure 6. Values are mean ± SEM, n=4, ***p < 0.001. (**B**) T24T cells were analyzed for clonal growth with 1% serum medium with or without macrophage-conditioned medium, with control or anti-CD44 antibody. Values are fold change relative to untreated cells, n=3, **p < 0.01. (**C**) Colony assays as in (A) were done using UMUC3 cells stably transduced with the indicated constructs. n=4, *p < 0.05. (**D**) UMUC3 cells transduced with scrambled or TIAM1 shRNA were analyzed for colony formation as in (A), n=4, *p < 0.05. (**E**) UMUC3 cells stably expressing GFP, GFP-GDI2 or GFP-GDI2D182R were analyzed for clonal growth with or without macrophage-conditioned medium as in (A), n=4, *p < 0.05. (**F**) T24 cells stably expressing scrambled or RhoGDI2 shRNA were analyzed for clonal growth with or without macrophage-conditioned medium as in (A), n=3, *p < 0.05. See also Figure S7.

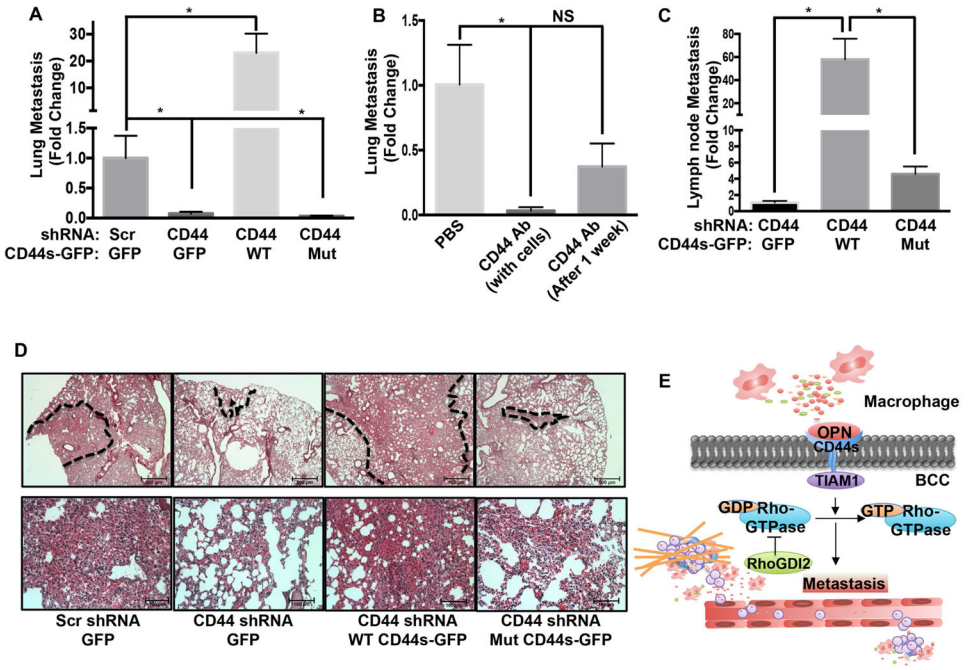

Figure 8. CD44 inhibition suppresses metastasis

(**A**) UMUC3 cells expressing the indicated shRNA and rescue vectors were injected into mice via the tail vein and metastasis assayed as described in experimental procedures. Values are mean ± SEM, fold change relative to control. Scrambled shRNA + GFP (n=11); CD44 shRNA + GFP (n=10); CD44 shRNA + WT CD44s-GFP (n=9); CD44 shRNA + Mut CD44s-GFP (n=10), *p < 0.05. (**B**) UMUC3 cells were injected with or without 50 μg/mouse anti-CD44 (hermes-1) antibody. For some mice, antibody injection started 1 week after cell injections. Lung metastasis was determined as in (A); Values are mean ± SEM, fold change relative to PBS. *p < 0.05, PBS (n=5), CD44 antibody with cells (n=5) and CD44 antibody after 1 week (n=5). (**C**) Luciferase labeled UMUC3 cells in which CD44 was stably depleted, were rescued with GFP only (control), WT CD44-GFP or Mut CD44-GFP. Cells were injected orthotopically and lymph nodes metastasis quantified as described in experimental procedures. Values are mean ± SEM, CD44 shRNA + GFP (n=7); CD44 shRNA + WT CD44s-GFP (n=8); CD44 shRNA + Mut CD44s-GFP (n=8), *p < 0.05. (**D**) Representative H&E images of mouse lung from the experiment described in (A). Areas of high metastasis marked with dotted line (upper panel, scale bar-500 μM) and higher magnification from marked area is shown in lower panel, (scale bar, 100 μM). (**E**) Graphical presentation of bladder cancer cells (BCC) and tumor microenvironment communication. See also Figure S8.